Regenerative potential of human enteric glia in a preclinical model of acute brain injury

Nina Colitti[a], Edwige Rice[a], Franck Desmoulin[a], Maylis Combeau[a], Mélissa Parny[b,c], Lorenne Robert[a], Etienne Buscail[d,e], Barbara Bournet[e], Nathalie Vergnolle[d], Isabelle Raymond-Letron[b,c], Isabelle Loubinoux[a], Carla Cirillo[a,#]

[a]ToNIC, Toulouse NeuroImaging Center, Inserm U1214, Toulouse University, UPS, Toulouse, France

[b]LabHPEC, Veterinary Histopathology Laboratory ENVT, Toulouse University, Toulouse, France

[c]RESTORE Institute, Inserm, Cnrs, EFS, ENVT, Toulouse University, Toulouse, France

[d]IRSD, Digestive Health research Institute, Inserm U1220, Toulouse University, UPS, Toulouse, France

[e]Department of Digestive Surgery, Toulouse University Hospital, Toulouse, France

[#]*Corresponding author:*
Carla Cirillo, PharmD, PhD, HDR
ToNIC, UMR1214 Inserm/UPS,
Hôpital Purpan, Pavillon Baudot,
Place du Dr Baylac
31024 Toulouse - Cedex 3
Tel: +33 5 62 74 61 87
Fax: +33 5 62 74 61 63
carla.cirillo@inserm.fr
http://www.tonic.inserm.fr/

Abstract

Acute brain injuries are characterized by extensive tissue damage, resulting in neuronal loss and severe functional deficits in patients. Self-regeneration is insufficient for the repair of damaged tissue. Therapies based on exogenous cells may offer a promising approach. In this study, we evaluated the feasibility of transplanting exogenous human enteric glia (hEG) in a preclinical model of brain injury. hEG were isolated, expanded and administered intranasally in brain-injured immunocompetent rats. hEG satisfied the safety criteria for cell therapy and were well tolerated. Additionally, hEG migrated to the injured area of the brain, where they enhanced endogenous angiogenesis and neurogenesis, contributing to tissue regeneration. Notably, hEG generated neurons that engrafted and integrated into the brain tissue. These neurons were enveloped by host oligodendrocytes and formed synaptic connections within the host tissue. Our findings provide evidence that hEG have regenerative potential and might be safely used for repair strategies in brain injury.

INTRODUCTION

Acute brain injuries, such as stroke and traumatic brain injury, are characterized by extensive damage to brain tissue, resulting in neuronal loss and functional deficits in patients, who are severely debilitated. Self-repair can occur through endogenous mechanisms, including neurogenesis, gliogenesis and angiogenesis, but these are dramatically limited, especially in adulthood*(1)*.

In recent decades, the use of stem/progenitor cells as a therapeutic strategy for brain tissue repair has been extensively tested in animal models, and, in some cases, in clinical trials in patients with stroke or injury*(2–7)*. Various cell sources have been investigated, including neural, embryonic, mesenchymal, and induced pluripotent stem cells *(8–12)*. While encouraging results have been obtained in animal models of brain injury, the translation of these findings to clinical application has proven to be challenging for several reasons. These include difficulties in choosing an appropriate route of administration, concerns about the safety, a high mortality rate and poor integration of donor cells into the host tissue, to ultimately restore functional deficits *(13)*. Despite considerable progress, the field has yet to identify an ideal donor cell population.

A suitable cell candidate should, in principle, be easily accessible, demonstrate high plasticity (for the generation of neurons) while simultaneously exhibiting a minimal risk to cause adverse outcomes. In addition, there is a need for a 'ready-to-use' cell source that does not require complex *in vitro* manipulation and high production costs.

The present study proposes an innovative cell source for brain repair, with the objective of overcoming the intrinsic issues associated with the utilization of current cell-based therapies. In humans, nerve tissue is not only present in the brain; it is also present in the periphery. The enteric nervous system (ENS), a highly organized network of neurons and glia cells in the gastrointestinal tract, may serve as a significant reservoir of transplantable cells*(14)*. Particularly, glia cells in the ENS have properties that make them interesting candidates for regenerative purposes. In humans, enteric glia (hEG) have important role in neuronal support, they display plasticity, and are safe with regard to immunogenicity and tumorigenicity*(15–22)*. In our previous studies, we have demonstrated that hEG can be accessed with relative ease from intestinal tissue and isolated to obtain pure primary cultures*(15, 18, 22)*. Importantly, in

comparison to stem/progenitor cells, we have shown that hEG can be readily expanded *in vitro* and cryopreserved, thereby allowing the quantities required for repair therapy to be obtained*(15)*. In this study, we tested the regenerative potential of hEG directly *in vivo*, in a rat model of acute brain injury, which was previously validated*(23)*. The model consists in the injection of a toxin, malonate, into the motor cortex, resulting in extensive tissue damage. This induces long-lasting functional deficits, thereby mirroring the clinical characteristics of acute brain injury in humans*(23–25)*. In injured animals, invasive cell transplantation induces exacerbation of tissue damage*(26–30)*. Intranasal delivery represents a viable alternative for the successful delivery of donor cells, which cross the cribriform plate and migrate *via* the rostral migratory stream to the brain*(31–33)*.

The present study shows that, following intranasal administration, hEG migrated to and successfully engrafted the brain tissue, where they generated neurons that were surrounded by host oligodendrocytes and formed synapses. Additionally, hEG enhanced tissue remodeling, endogenous angiogenesis, and neurogenesis, thus contributing to the regeneration of brain tissue.

RESULTS

The study protocol is shown in *Figure 1*. We had four groups of rats (hEG, vehicle, hEG-conditioned medium, and medium alone), in which the animal's behavior, brain anatomy (*in vivo* analysis), tissue regeneration and remodeling in brain slices (*post-mortem* analysis) were investigated. The strategy of using hEG-conditioned medium or medium alone allowed for the exclusion of potential effects due to factors other than cell delivery. By reason of clarity, it should be noted that the temporal discrepancy between the final MRI and the sacrifice was due to the constraints imposed by the Coronavirus pandemic, which necessitated a modification of the original plan.

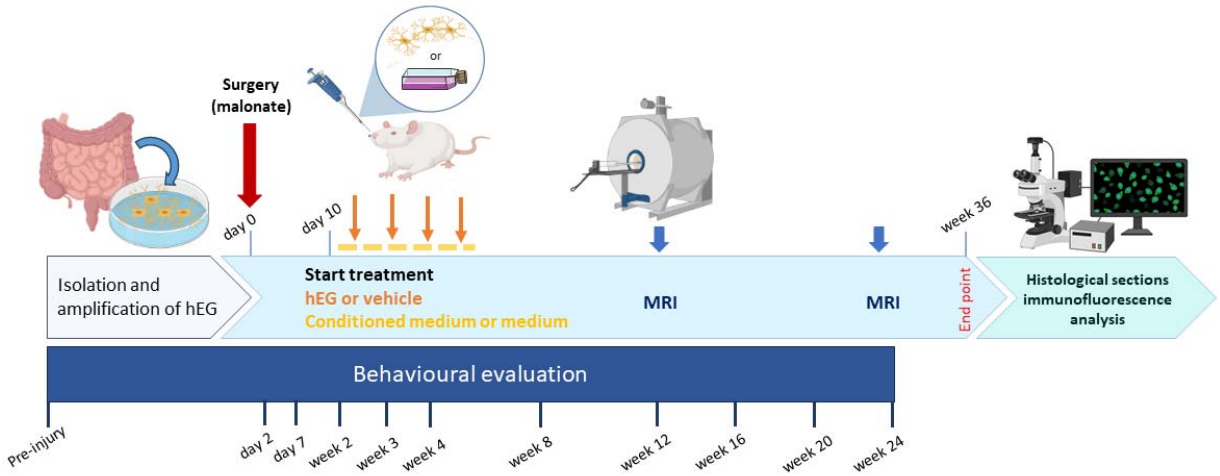

***Figure 1**: Detailed study protocol.* Behavioral tests started before injury and were performed at different time points: day 2, day 7 and week 2, 3, 4, 8, 12, 16, 20 and 24 post-injury. Brain injury was induced in adult female rats (*n=28*, 12-week-old) by malonate injection into the cortex (*red arrow*). Ten days after the injury, rats received hEG (*n=7*) or vehicle (*n=7*) intranasally, once/week for a month (*orange arrows*; $2.5x10^5$ cells/administration). The two other groups of rats received conditioned medium (*n=7*) or medium (*n=7*) ten days after injury every day for a month (*yellow dashes*). MRI acquisitions were performed 12 weeks and 24 weeks post-injury. Histological analysis was performed 36 weeks post-injury, to assess tissue regeneration, host cell reorganization, and to identify cell populations. MRI: magnetic resonance imaging. hEG: human enteric glia.

In vitro characterization of the purity of hEG cultures

Mature hEG were isolated from the myenteric plexus of the gut and amplified as we previously established*(15, 18, 22)* (detailed in *Supplementary M&M*). After five passages, before the administration in brain injured rats, hEG cultures were characterized by immunostaining to assess their purity. We evaluated the protein expression of glial specific markers: GFAP, S100, SOX10, which were all expressed in mature hEG (*Figure 2A-C*). As expected, primary cultures did not express fibroblast (α-SMA) (*Figure 2C, middle*) or neuronal markers (HuC/D and NeuN) (*Figure 2D-E*). These results demonstrated the purity of hEG cultures and the absence of contaminating cells, like neurons or fibroblasts, confirming our previous studies*(15, 18, 22)*. In addition, we investigated whether mature hEG in culture possessed neurogenic property. The expression of the transcription factor ASCL1 (Mash1), which regulates enteric neurogenesis*(34)*, demonstrated that mature hEG have neurogenic potential (*Figure 2F*) and indicated that mature hEG do not need *in vitro* reprogramming to acquire their neurogenic potential.

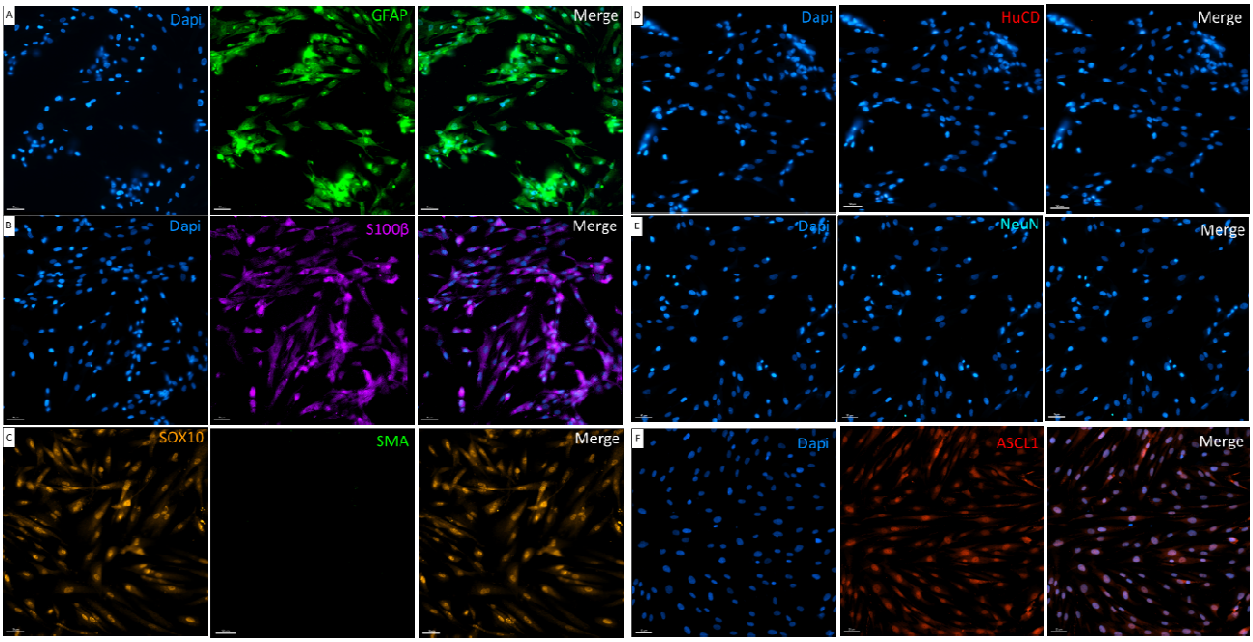

***Figure 2**: Immunostaining of hEG cultures.* hEG in culture shown typical glial morphology. (A) Images showing Dapi labelling (left), GFAP positive labelling (middle) and merge (right). (B) Immunostaining of hEG showing Dapi labelling (left), S100ß positive labelling (middle) and merge (right). (C) Immunostaining of hEG showing positive nuclear SOX10 labelling (left), negative SMA labelling (middle) and merge (right). (D) Immunostaining of hEG showing Dapi labelling (left), negative HuCD labelling (middle) and merge (right). (E) Immunostaining of hEG showing Dapi labelling (left), negative NeuN labelling (middle) and merge (right). (F) Immunostaining of hEG showing Dapi labelling (left), positive nuclear ASCL1 labelling (middle) and merge (right). Scale bars: 50 µm. GFAP: Glial Fibrillary Acid Protein, S100ß: S100 intracytosolic calcium binding protein, SMA: alpha skeletal muscle, HuCD:

neuron-specific RNA-binding protein, NeuN: Neuronal nuclei marker, ASCL1: Achaete-Scute Family BHLH Transcription Factor 1.

Intranasal administration of hEG shows long-term safety in immunocompetent rats

The observation of clinical signs provided regular monitoring of the animals after brain injury and intranasal administration throughout the study. The animals receiving hEG showed no signs of local or systemic toxicity, indicating that they tolerated well the treatment with exogenous human cells (xenograft). This is an important finding given that our rats were immunocompetent. To further assess the safety of our therapeutic strategy, we used appropriate behavioral tests.

The *emergence test* provides information on anxiety state. The injection of malonate in the motor cortex increased the latency to exit the dark compartment one-week post-injury in all rats *($p<0.0001$, Figure 3A*). As expected, the latency time was markedly diminished in all groups eight-week post-injury *($p<0.05$, Figure 3A*), continuing until the twenty-four-week interval.

The *neurological severity scale (NSS)* assessed the sensorimotor deficit measured with a scoring ranging from 0 to 16. *Figure 3B* shows a significant increase (*$p<0.01$*) in the score two days post-injury, reflecting the consequences of the lesion in the sensorimotor cortex. The rats recovered from twelve weeks post-injury onwards. A *plateau* was reached at twelve weeks. Statistically, there was no difference among the four groups.

The *limb-use asymmetry test* evaluated the spontaneous use of the front limbs. It measures the deficit of the whole limb including shoulder, elbow, and paw. The asymmetry corresponds to the difference between the use of the ipsilateral - contralateral paw compared to the number of supports, in percentage. Non-injured rats made simultaneous elevation against a support or used their dominant paw. As expected, the percentage of asymmetry increased in all groups one-week post-injury (*$p<0.05$, Figure 3C*). There was no significant effect among the four groups.

The *grip test* measures the grip strength of the forelimbs and was used to identify the dominant paw in each animal. The percentage of contralateral paw strength is shown in *Figure 3D*, after injury and after intranasal delivery of treatments. Rats in all four groups were deficient two days after injury. The mixed-effects analysis multiple comparison test compares the values measured two days post-injury to the pre-injury for the vehicle group ($p=0.012$), hEG group ($p=0.001$), medium group ($p=0.034$) and conditioned medium group ($p=0.006$). The recovery for vehicle and medium groups flattened to the top after spontaneous recovery (*Figure 2D*), as previously

reported*(23, 24)*. Rats receiving conditioned medium showed functional recovery comparable with the group receiving medium alone. Interestingly, the rats receiving hEG showed a good improvement in strength compared with vehicle group, with a better delta recovery calculated between eight and twenty-four weeks, *(t(9)= 2.72, p=0.023; IC_{95}= [3.943-42.72], Figure 3D')*.

Together, behavioral tests indicated that all groups tolerated the treatments well, showing no worsening of the deficits. Importantly, in the group receiving hEG, no side effects on behavior were observed throughout the study, and the animals exhibited the expected spontaneous recovery over time.

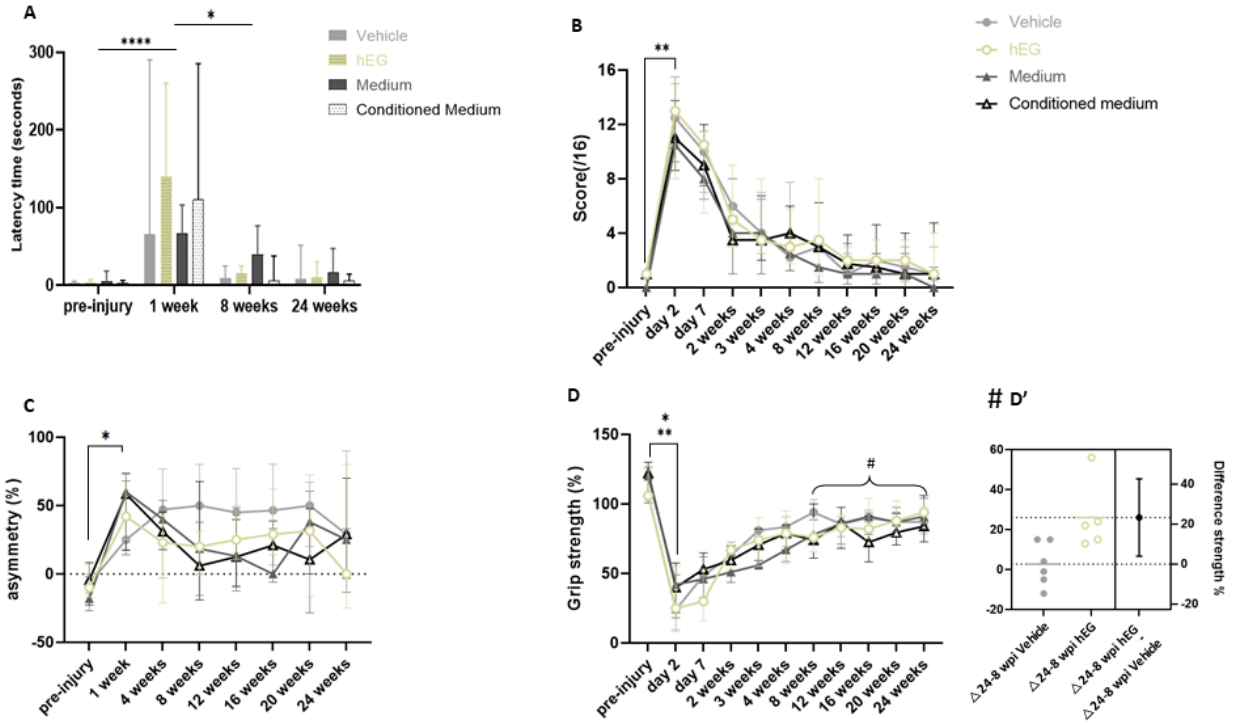

***Figure 3**: Effect of intranasal administration on behavioral tests.* (A) The anxiety test measuring the latency to remove two paws from a black box. The latency was significantly increased one-week post-injury for all the groups (mixed-effects analysis multiple comparison test, ****p<0.0001). The latency significantly decreased between 1 week and 8 weeks post-injury in all groups, independently of the treatment (*p<0.05). (B) The neurologic scale score measures sensory-motor impairments (score out of 16). The four groups were significantly impaired 2 days post-injury (mixed-effects analysis multiple comparison test **p<0.01). (C) The limb-use asymmetry test measures the asymmetric use of the limb. The four groups were significantly impaired on the contralateral limb one-week post-injury (mixed-effects analysis multiple comparison test *p<0.05). (D) The grip strength test shows the grip strength of the front paw contralateral to the injected hemisphere compared to the other paw, expressed as %. Rats in all four groups were deficient two days after injury (*Wilcoxon test, p<0.05*). (D') The graph shows the 95% confidence interval: [3.943 to 42.72] with a difference strength of 26% for hEG group and 2.6% for vehicle group

between 8 weeks and 24 weeks. For (A–D): *n=7* per group; wpi: weeks post-injury. The median and the interquartile range are represented.

In vivo characterization of brain injury

MRI was performed twelve- and twenty-four weeks post-injury (*Supplementary Figure 1A and B*). T2-weighted images allowed to visualize hyperintense, vasogenic and cytotoxic edemas. Lesions are characterized by an increase in T2 signal. Twelve weeks post-injury, the distribution of lesion volumes in matched groups have similar medians: vehicle=79.15mm^3 *vs* hEG=69.86mm^3; medium=42.87mm^3 *vs* conditioned medium=43.92mm^3 (*Supplementary Figure 1C*). The same tendency was measured twenty-four weeks post-injury, where the distribution of lesion volumes in matched groups have similar medians: vehicle=121.10mm^3 *vs* hEG=94.15mm^3; medium=55.50mm^3 *vs* conditioned medium=51.72mm^3 (*Supplementary Figure 1D*). Regarding the distribution of atrophy in percentage, 24 weeks post-injury, the hEG group showed a reduced percentage, although not statistically significant, compared with the other groups: vehicle=6.20%; hEG=3.35%; medium=12.02%; conditioned medium=15.14% (*Supplementary Figure 1E*).

Exogenous hEG sustain brain tissue regeneration

Histological analysis using Nissl staining was used to appreciate and quantify the new tissue in the damaged brain area. In a recent paper, we developed a method for quantifying this tissue*(23)*. *Figure 4* shows the characterization of the new tissue in the four groups of rats; the dotted black line corresponds to the lesion and the dotted red line identifies the new tissue. Daily injection of conditioned medium for one month did not promote the formation of new tissue (7% *vs*. 15% in medium group). In contrast, intranasal administration of hEG induced a remarkable tissue regeneration, as shown in *Figure 4B, B' and E*. Strikingly, the quantification of the new tissue reached 24% for hEG *vs*. 10% for vehicle group (*Figure 4E, p=0.016*). An interesting finding was the fact that, when we looked at each animal in detail, we found that in the hEG group one rat with small lesion size had a high percentage of reconstructed tissue (51.0%, *Supplementary Figure 2A, B and E*). This was associated with important rescue of sensorimotor deficits, especially for the asymmetry test (*Supplementary Figure 2F-H*). We compared this rat with one having similar lesion size but receiving the vehicle. As expected, we found lower tissue regeneration (10.5%, *Supplementary Figure 2C-E*), with negligible restoration of sensorimotor

deficits (*Supplementary Figure 2F-H*). This result suggests a link between the extent of tissue regeneration and rescue of sensorimotor impairment.

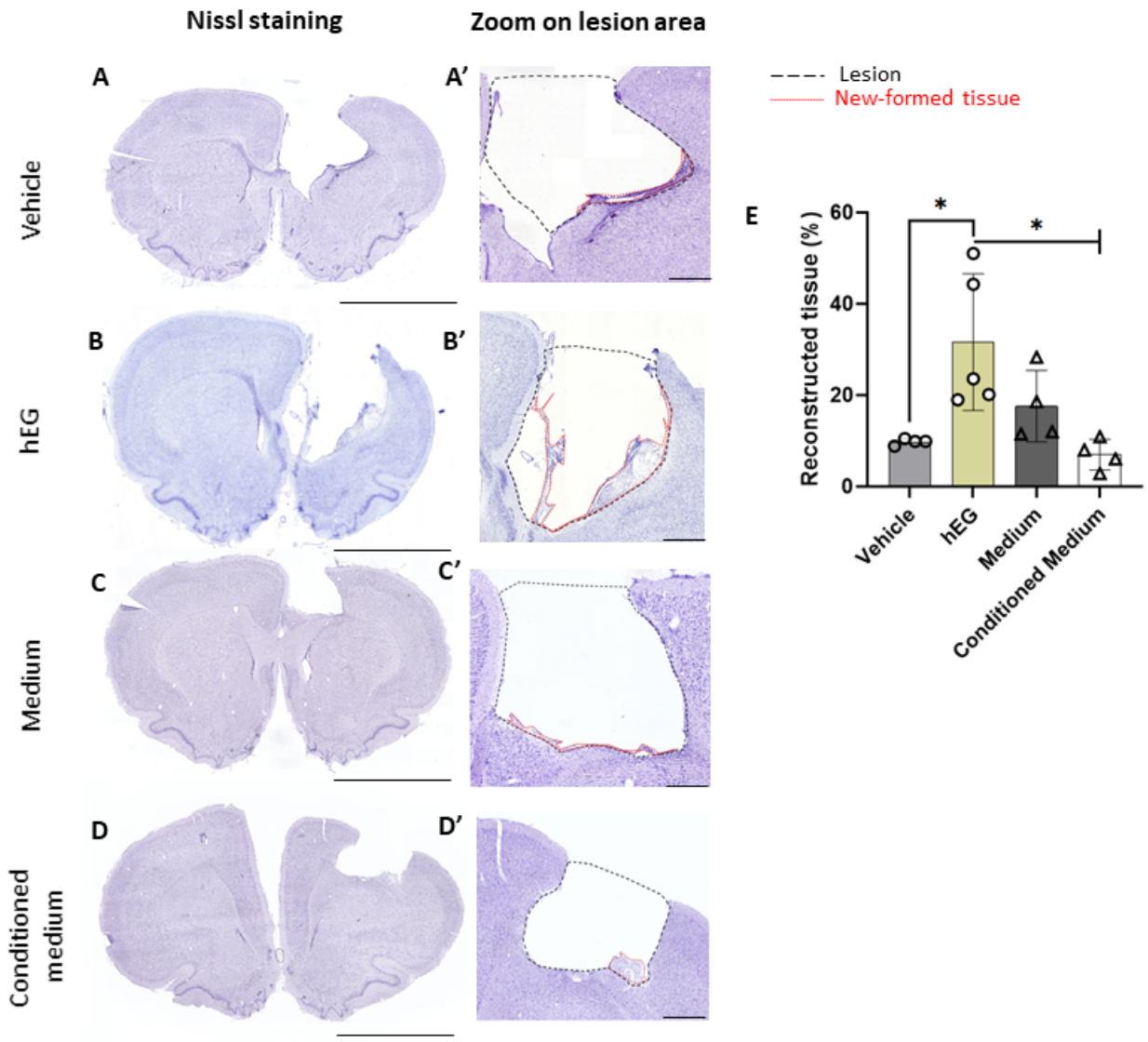

***Figure 4**: New tissue quantification and characterization*. (A) Nissl staining on coronal section in rat receiving vehicle. (A') Magnification showing the edges of the lesion (black dashed lines) and the new tissue (red dotted lines) 24 weeks post-injury in vehicle group. (B) Nissl staining in rat receiving hEG. (B') Magnification showing the edges of the injury and the new tissue 24 weeks post-injury in hEG group. (C) Nissl staining in rat receiving medium. (C') Magnification showing the edges of the lesion and the new tissue 24 weeks post-injury in medium group. (D) Nissl staining in rat receiving conditioned medium. (D') Magnification showing the edges of the injury and the new tissue 24 weeks post-injury in conditioned medium group. (E) Graph showing the quantification of the new tissue normalized by the lesion volume in the different groups. The percentage of new tissue was significantly increased in rats receiving hEG (#p=0.016 *vs* vehicle group, and *p=0.016 *vs* conditioned medium group, Mann Whitney test). The median and the interquartile range are represented. Vehicle group: *n=4*; hEG group: *n=5*; Medium group *n=4*; Conditioned medium group *n=4*. A, B, C, D scale bars: 5 mm; A', B', C', D' scale bars: 500 µm.

Exogenous hEG induce host tissue remodeling

Markers of inflammation were quantified to evaluate the response to the four experimental conditions. Intranasal administration of hEG had no effect on astrocytes (Gfap$^+$, *Figure 5A-F*) and microglia (Iba1$^+$, *Figure A, G-K*) infiltration, compared with the other three groups. The staining with Gfap also allowed measuring the thickness of the glial barrier at the edge of the lesion. The glial barrier is a hallmark after brain injury and is mainly formed of astrocytes. Although we did not find a statistically significant difference in barrier thickness in the four groups, we observed a different architecture of this in rats receiving hEG (*Figure 5L-P*), in which the astrocyte barrier appeared loose and less dense, with palisading astrocytes (*Figure 5M*). These results indicate that hEG are able to induce the remodeling of the injured tissue by reducing the typical tissue hallmarks of brain injury.

Angiogenesis is another important criterion of tissue remodeling. Indeed, neovascularization is a positive criterion for the evolution of lesions, which tends more towards regeneration than cicatrization. We assessed the extent of neovessels using the endothelial cell marker Lectin. The quantification of vessel surface revealed enhanced neovascularization in the hEG group compared with the other groups (2.3×10^4 µm^2, p=0.029, *Figure 6A-F*). Interestingly, in the hEG group, the neovessels were found extending into the new tissue (*Figure 6C*).

Further, we evaluated endogenous neurogenesis in the host tissue using three markers corresponding to the different stages of neuronal differentiation: doublecortin (DCX) for neuronal progenitors, betaIII tubulin (βIIItub) for immature neurons, and NeuN for mature neurons. In all groups, we observed the presence of DCX$^+$ cells in the new tissue, indicating the migration of neuronal progenitors from the subventricular zone (SVZ, neurogenic niche) *(Figure 6G-K)*. This suggests that, in our brain injury model, the neurogenesis process was still present thirty-six weeks post-injury. Outstandingly, intranasal administration of hEG induced an increase in both mature (NeuN: 35% *vs*. 11% in vehicle group, p=0.029, *Figure 6Q-U*) and immature neurons (βIIItub: 24% *vs*. 9% in vehicle group, p=0.029, *Figure 6L-P*), in the new tissue. These results indicate that exogenous hEG importantly contributed to tissue remodeling and enhanced endogenous angiogenesis and neurogenesis.

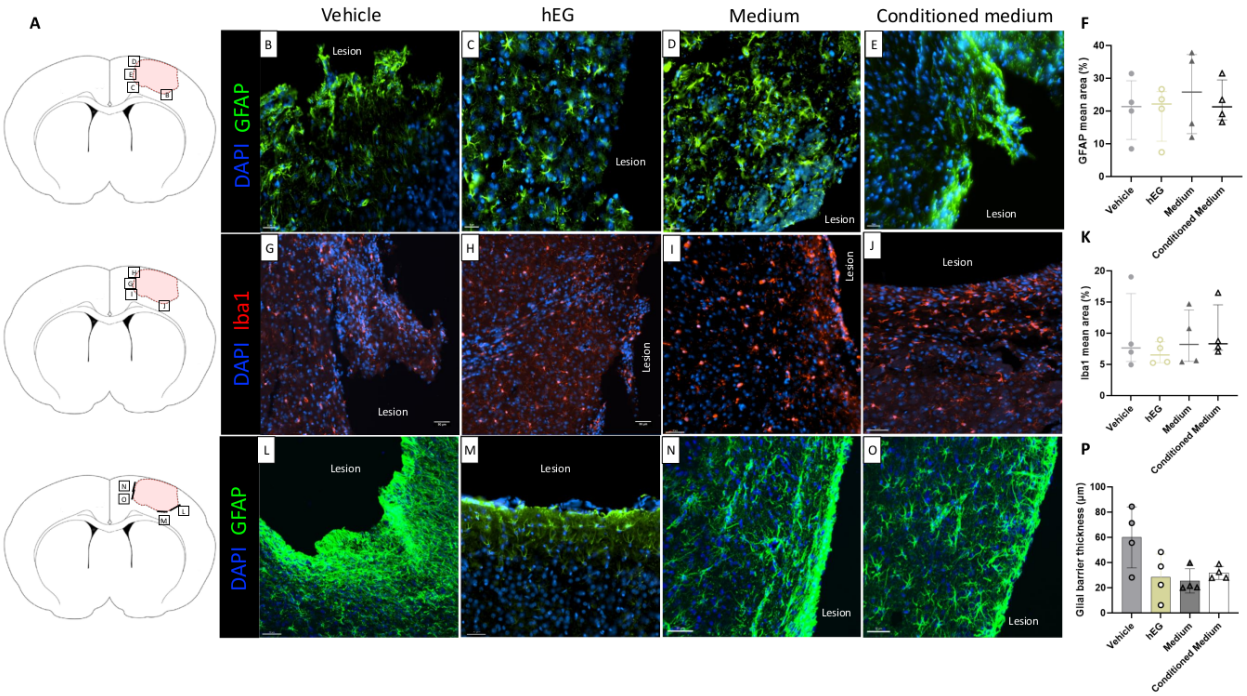

***Figure 5**: Characterization of the inflammation in the new tissue and at the edge of the lesion 36 weeks post-injury.* (A) Location of illustrated areas in B-O. (B-F) Representative images and quantification of GFAP (to identify astrocytes) in the new tissue. (G-K) Representative images and quantification of Iba1 (to identify microglia) in the new tissue. There was no significant difference in the number of immune cells between the groups, as reported in the graphs. (L-P) Representative images and quantification of the astroglial barrier (expressed in µm) based on GFAP mean intensity (fluorescence) in the different groups. There was no significant difference between the groups. All graphs show the distribution of individual values and the median ± the interquartile range. For all groups, *n=4*. Scale bars B-E: 30 µm; G-O: 50 µm. GFAP: glial fibrillary acidic protein.

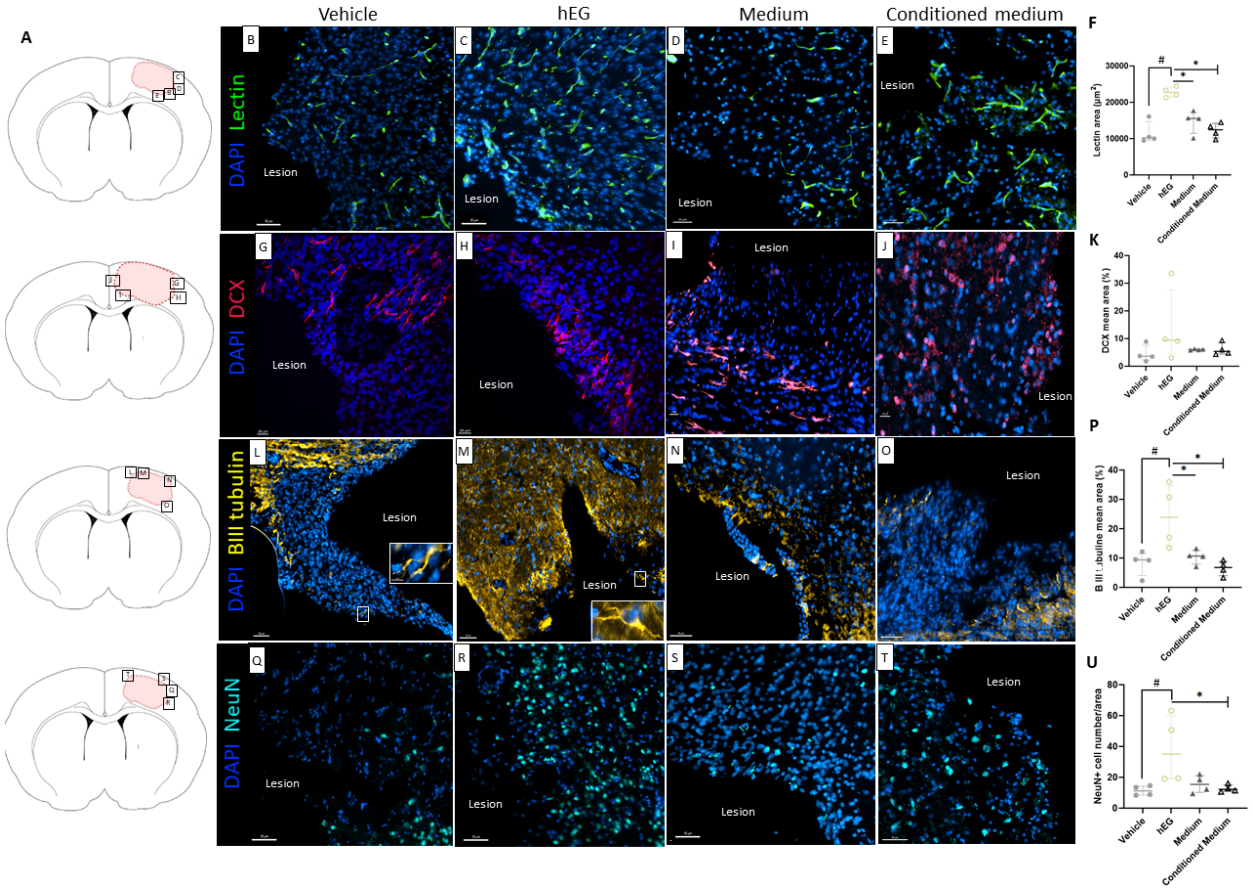

***Figure 6**: Characterization of the endogenous angiogenesis and neurogenesis in the new tissue 36 weeks post-injury*. (A) Location of illustrated areas in B-T. (B-F) Representative images and quantification of Lectin (identify blood vessels) in the new tissue. Positive surface of Lectin is increased in rats receiving hEG compared to the other groups #*p=0.029. (G-K) Representative images and quantification of Doublecortin (identify progenitor neurons) in the new tissue. (L-P) Representative images and quantification of ßIII tubulin (identify immature neurons) in the new tissue. The inserts show positives ßIII tubulin cell (white arrowheads). A significant difference in the percentage of ßIII Tubulin between vehicle and hEG group was observed (#p=0.029), also between conditioned medium and hEG group (*p=0.029), and between medium and hEG group (*p=0.029). (Q-U) Representative images and quantification of NeuN (to identify mature neurons) in the new tissue. A significant difference of NeuN-positive cells between the vehicle and hEG group was observed (#p=0.029), also between the conditioned medium and hEG group (*p=0.029). Mann-Whitney tests were performed. All graphs show the distribution of individual values and the median ± the interquartile range. For all groups, *n=4*. Scale bars G-J: 20 µm; B-E and L-T: 50 µm. DCX: Doublecortin, NeuN: neuronal nuclei.

Intranasally administered hEG migrate to the lesion area, but do not over proliferate

Following the observation that hEG administration had a beneficial impact on the evolution of the injured tissue, in the subsequent phase of the study we focused on rats receiving hEG and compared them with the vehicle group.

The staining with the human specific nuclei marker, shown in red in *Figure 7*, enabled the identification, localization, and quantification of human transplanted cells after intranasal administration (*Figure 7A-E*). Intriguingly, human transplanted cells were identified thirty-six weeks post-injury, which demonstrates their long-term survival. This is an important requisite for cell-based therapy. The quantification of these cells revealed a density gradient-like distribution (*Figure 7F*) of human cells in the host brain, with a higher number of cells in the injured site (ipsilesional cortex) compared to the healthy hemisphere (contalesional cortex) (*Figure 7D and E*, respectively). Further, higher numbers of human nuclei-positive cells were identified at the lesion site corresponding to bregma level 2 to 0 slices (median: 4597.5 human nuclei^{+} cells/slice, *Figure 7F*). Interestingly, transplanted cells did not remain in the olfactory bulb or in the frontal region (data not shown), nor were they detected in the region caudally to the lesion site (*Figure 7F*). Together, these findings indicate that transplanted hEG migrated, survived, and integrated into the host brain, preferentially but not exclusively, in the injured site.

By reason of the long duration of the study, we wanted to verify the absence of tumorigenic effect after the administration of exogenous hEG. Thus, we evaluated the expression of classic markers of proliferation. Ki67 MIB1 corresponds to the proliferation marker specific to human cells, allowing us to determine whether exogenous hEG were proliferating into the host brain. No Ki67 MIB1^{+} human cells were observed in brain sections (*Figure 7I-I'*). This is an important finding, as it underlines the safety of exogenous hEG. In parallel, we evaluated the proliferation rate of host (rat) cells, by using Ki67 B56, which labels cycling cells. We found Ki67 B56^{+} cells in the two groups of rats (*Figure 7G-G' and H-H'*) and we quantified them at the edge of the ventricles, which served as a control of proliferative area (*green arrow*), and in the new tissue (*dark arrow*). Along the ventricles the percentage of cells was comparable in the two groups (24.5% in vehicle group, 21.2% in hEG group, *Figure 7J*); however increased numbers of proliferating cells were evident in the new tissue for the group receiving hEG (12.4% *vs*. 8.8% in vehicle group, *Figure 7J).* The findings demonstrate that tissue remodeling is still ongoing thirty-

six weeks post-injury; however, no evidence of tumorigenic risk related to the administration of hEG was found.

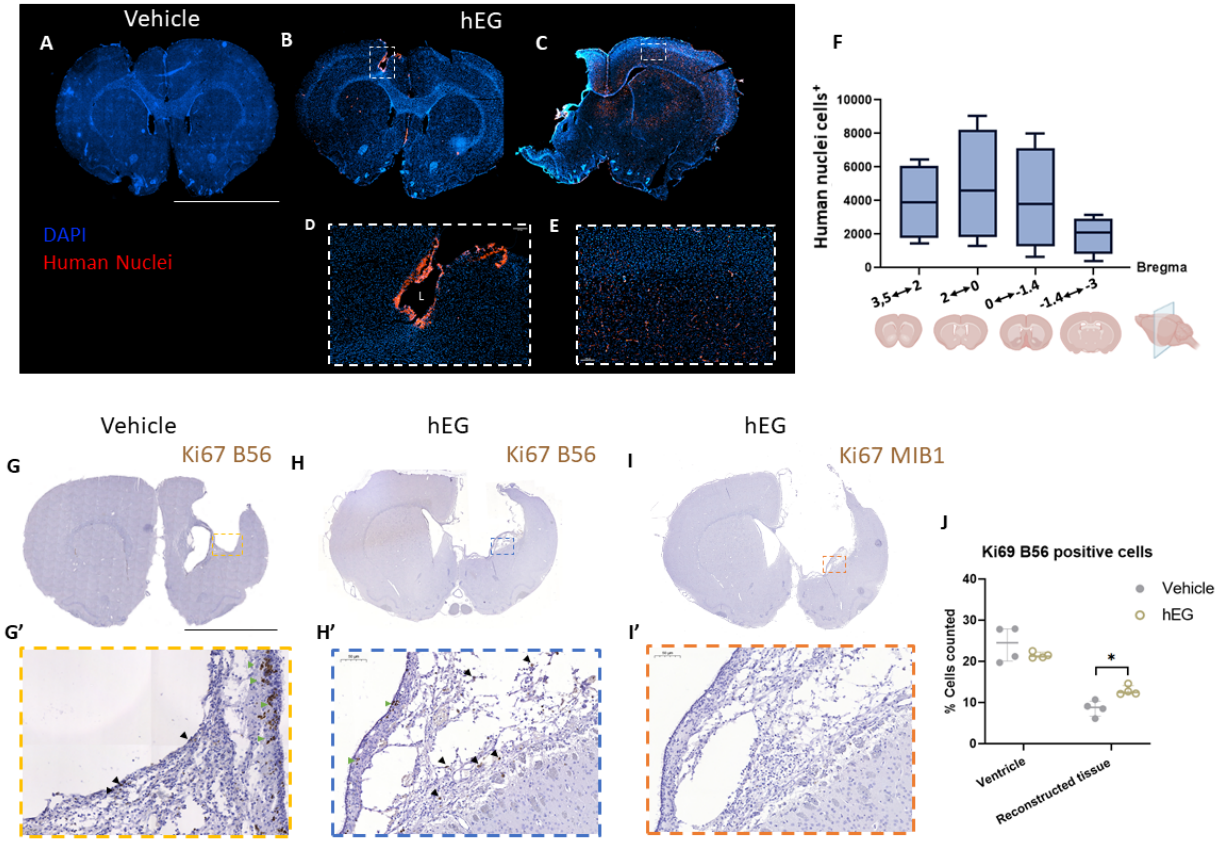

Figure 7: *Identification, location, and quantification of hEG 36 weeks post-transplantation*. (A) Coronal brain section of rat receiving vehicle. Negative control for Human nuclei antibody. (B-E) Coronal brain section of rats receiving hEG. Representative images showing human cell location. (F) Quantification of hEG in brain sections from 3,5mm bregma to -3mm bregma. Data for each notch box are represented as median ± interquartile range of twelve slices obtained from *n=4* rats. A total of 48 sections were quantified. *Proliferation rate of human and rat cells*. (G-H) Representative images of Ki67-B56 staining for vehicle group (G) and hEG group (H). Magnification reveals positive host cells in proliferation (brown). (I) Representative image of Ki67-MIB1 staining for the hEG group, showing no human cells positive for the proliferation marker. (J) Ki67 positive cell quantification in selected regions of interest with representative images from ventricle (green arrows) and new tissue (dark arrows). Data are represented as individual values with median ± interquartile range. The % of positive Ki67 B56 cells was increased in the new tissue in rats receiving hEG (Mann Whitney test *p=0.028). Ki67-B56: Rat specific marker of proliferation; Ki67-MIB1: Human specific marker of proliferation. Scale bars (A-C, G-I): 5 mm; scale bars (D, E): 150 µm; scale bars (G'-I'): 50 µm, L=lesion.

Exogenous hEG generate neurons that integrate into the host brain tissue

To determine the fate of hEG following their arrival in the injured brain, we used the STEM121 antibody, which specifically labels the cytoplasm of human cells. Compared to human nuclei staining, STEM121 allowed to appreciate the morphology of positive cells. We observed that STEM121$^+$ cells had a neuronal-like body, as shown in the ipsilesional area (*Figure 8A and B, left*). To confirm our hypothesis, we double-stained brain slices with the neuronal specific marker NeuN, which labels mature neurons, and quantified them. Impressively, we detected 95% of double STEM121$^+$/NeuN$^+$ cells (*Figure 8B and E, middle and right, white arrowheads*). As depicted in *Figure 8B* (*yellow arrowhead*), some STEM121$^+$ neurons showed the morphology of an interneuron. Double STEM121$^+$/NeuN$^+$ cells were detected as well in the contralesional area (*data not shown*). In parallel, we used glial specific markers Gfap and S100 to evaluate whether hEG retained their glial nature once in the injured brain. We found that only a few cells (5%) were double STEM121$^+$/S100$^+$ or STEM121$^+$/Gfap$^+$ (*Figure 8E and Supplementary Figure 3*).

In order to evaluate the successful anatomic integration of hEG-derived neurons into the host brain, we used two specific markers: the Osp (oligodendrocyte-specific protein) marker for myelin and the synaptophysin marker for synapses. Excitingly, hEG-derived neurons were integrated and aligned in a neat pattern into the brain cortex and were surrounded by host oligodendrocytes (Osp$^+$ cells), indicating that they were myelinated (*Figure 8C*). The alignment and support by oligodendrocytes are clearly appreciable in the 3D image reconstruction *(movie V1)*. Additionally, we found positive synaptophysin staining around STEM121$^+$ cells, which indicated the formation of synapses, a marker of neuronal connectivity *(Figure 8D)*. These findings show the robust integration of hEG-derived neurons into the host tissue.

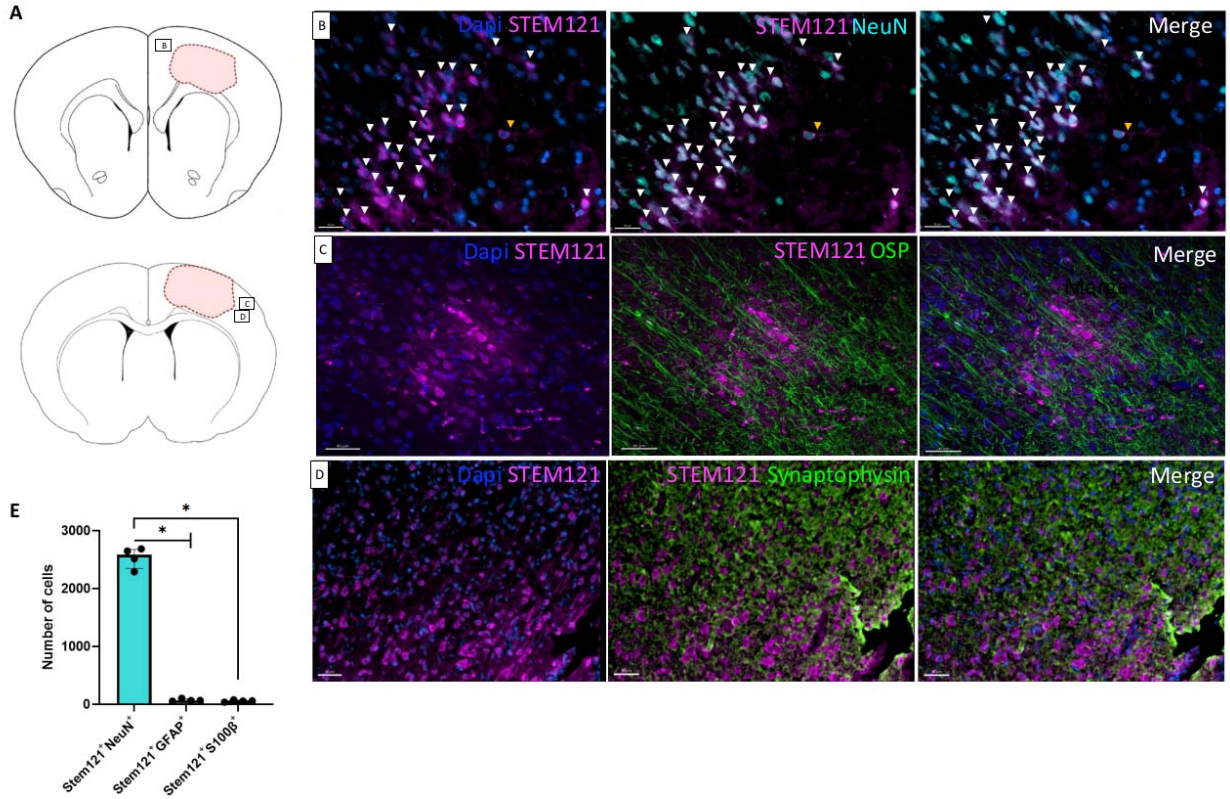

***Figure 8**: hEG generated neurons anatomically integrated into the injured brain*. (A) Location of illustrated areas. (B): Representative images of hEG stained with human cytoplasmic marker STEM121 and neuronal nuclei NeuN (double-positive: white arrow). The yellow arrow indicates a double-positive cell with an interneuron morphology. Left: Dapi and STEM121 staining, middle: STEM121 and NeuN staining, right: merge. (C) Representative images of intranasal hEG stained with human cytoplasmic marker STEM121, and oligodendrocytes with Osp marker specific for myelin. Left: Dapi and STEM121 staining, middle: STEM121 and Osp staining, right: merge. (D): Representative images of hEG stained with human cytoplasmic marker STEM121 and Synaptophysin, marker for presynaptic vesicles in neurons. Left: Dapi and STEM121 staining, middle: STEM121 and Synaptophysin staining, right: merge. (E) Graph showing the number of engrafted cells positive for neuronal marker: $STEM121^+/NeuN^+$ or glial marker $STEM121^+/GFAP^+$ or $STEM121^+/S100\beta^+$ (*p=0.029, Mann Whitney test). Individual values and the median ± the interquartile range are represented. Four counting frames (645 x 628 μm^2) for two sections per rat were quantified for *n=4* receiving hEG. A total of 32 fields were quantified.

DISCUSSION

This is the first study to demonstrate the safety and regenerative potential of hEG for the treatment of brain injury. Notably, we show that hEG migrated, survived, integrated into the rat brain tissue, and generated neurons. hEG-derived neurons were myelinated and established synaptic connections with the host tissue. Furthermore, hEG enhanced tissue remodeling, endogenous neurogenesis, and angiogenesis. Together, these effects resulted in marked tissue regeneration.

The evaluation of the safety and efficacy of cell therapies in valuable animal models of brain injury is an essential prerequisite for the translation into clinical trials. In this study, we used a rat model of brain injury that induces long-lasting sensorimotor deficits, mimicking the clinical signs of acute brain injury in humans*(23, 24)*. Two unprecedented aspects of our study are the fact that our rats were immunocompetent and the long duration of the protocol, up to thirty-six weeks. This strategy allowed us to assess that there were no side effects associated with hEG xenotransplantation. Specifically, the evaluation of clinical signs (observation) and brain tissue anatomy (MRI in live animals and *post-mortem* histology in brain slices) showed no evidence of toxicity in rats receiving hEG.

The integration of transplanted cells with the host tissue is a gradual process that may require considerable time to establish functional connections and, ultimately, functional recovery. In our model of long-lasting deficits, we observed a marked improvement in functional recovery, particularly in the grip test, between eight and twenty-four weeks in rats receiving hEG. However, no significant differences were appreciable for the other behavioral tests.

Given the human origin of the donor cells used in our study, assessing the inflammation around the injury and in the new tissue was essential. The evaluation of glial barrier*(35)* and microglial infiltration*(36–38)*, showed that, compared to the other groups, hEG delivery did not exacerbate these signs. In support of these findings regarding the safety of adult hEG, the utilization of a human specific cell marker, Ki67 MIB1, did not evince any indications of human cell proliferation thirty-six weeks following their administration. Conversely, the proliferation of host cells, identified with Ki67 B56 in the group receiving hEG, was observed in the new tissue, but not in other regions. Collectively, these findings substantiate that hEG safely participate in tissue remodeling.

The remodeling of injured tissue is necessary for effective tissue regeneration after brain injury*(39)*. Interestingly, in our study, the organization of astrocytes forming the glial barrier, was found to be permissive in rats that received hEG, in comparison to the other groups. This was due to the orientation of astrocytes, which appeared palisading. Together, these findings confirmed that the administration of hEG significantly contributed to tissue remodeling.

In this context, and in order to establish the therapeutic potential of hEG in our model of brain injury, it was essential to quantify the new tissue. Interestingly, we found 24% of new tissue following the administration of hEG, in comparison to 10% in the vehicle group. This percentage represents a remarkable degree of regeneration in relation to the lesion volume. To date, no other studies have quantified the reconstructed tissue following cell transplantation in the injured brain, preventing a comparison of our finding with other results.

The potential for quantifying new tissue also permitted the correlation of this parameter with other variables, such as the recovery of sensorimotor deficit. Interestingly, in the hEG group, the highest percentage of new tissue (51%) was found in a rat with a small lesion size, and this regeneration correlated with significant functional recovery compared to a rat in the vehicle group with a comparable lesion size. The detailed analysis indicated a notable recovery of motor function, particularly evident in the asymmetry test. This is intriguing, as the asymmetry test focuses on shoulder movement, thus revealing early motor improvements*(40, 41)*.

The observed functional improvement can be attributed to the presence of the new tissue. Given the limited size of the injury in this rat, we hypothesize that the dose of hEG (1×10□ hEG) was effective to induce substantial tissue regeneration, which was accompanied by quantifiable functional recovery. Most studies testing the feasibility of intranasal delivered cells in brain injury models have used about one million cells*(42–45)*. For example, Vanessa Donega's study in young mice tested different doses of MSCs ten days after injury*(46)*. They found that doses of 0.5×10□ and 1×10□ MSCs improved sensorimotor function, but a lower dose of 0.25×10□ did not*(46)*. We selected a dose (1×10□ hEG) that was consistent with the aforementioned studies. Modifying the number of transplanted cells in accordance with lesion size might have a greater effect on functional recovery. However, this hypothesis needs to be confirmed by the use of different doses of cells and the implementation of longer-term behavioral assessments.

The increase in reconstructed tissue observed in the hEG group could be due to increased host cell proliferation, as evidenced by positive staining for the specific marker Ki67-B56. This proliferation was characterized by enhanced endogenous angiogenesis (lectin$^+$ cells) and neurogenesis (βIIITub$^+$ and NeuN$^+$ cells). The combined effects of increased cell proliferation, angiogenesis and neurogenesis induced by hEG collectively contributed to the remarkable tissue regeneration observed in our study.

A noteworthy finding of our study is the migratory capacity of hEG, which makes the intranasal pathway particularly advantageous to the transplantation of these cells. Human nuclei$^+$ cells were detected mainly at the lesion site, but also across brain sections (rostral to caudal), exhibiting a gradient-like distribution. The quantification indicated a median value of human nuclei$^+$ cells per slice of 3 000, with a total of 20 000 positive cells counted in eight slices per rat, representing a percentage of 18.8% (median value) of intranasally delivered hEG. This result is remarkable in the context of cell-based strategies. Indeed, one of the limitations of other cell sources, such as stem or progenitor cells, is their clearance after transplantation. Only two articles identified in the literature made a quantification after local graft of neural stem/progenitor cells*(47)*, or ENS-derived progenitor cells*(48)* in mice with irradiation-induced brain injury. The first one found 3.6% of the total number of injected cells five months after cell transplantation*(47)*, while the second one identified only 0.1% of donor cells sixteen weeks after transplantation*(48)*. In our study, hEG were administered intranasally, necessitating the cells to migrate to the injured region of the brain, in contrast to the aforementioned studies which used local injection, which makes our finding notable.

Outstandingly, within the injured brain, we identified hEG-derived mature neurons, STEM121- and NeuN-positive cells, which accounted for 95% of total STEM121-positive cells. This was the most notable outcome of our study, clearly demonstrating the regenerative potential of hEG *in vivo*. In contrast, we found that only 5% of human cells retained their glial nature (GFAP- or S100-positive) in the injured brain. Interestingly, no double positive βIIITub/STEM121 or DCX/STEM121 cells were detected, suggesting that, thirty-six weeks post-injury, exogenous hEG did not exhibit a neuronal progenitor/immature nature. These *in vivo* data were supported by the *in vitro* evidence that primary mature hEG expressed the ASCL1 transcription factor, indicating their neurogenic potential, without the need of reprogramming. This is an important advantage, compared to other cell sources used for regenerative purposes*(48–51)*. To date, the

neurogenic potential of ENS glia has been described in the mouse intestine, where they may undergo neuronal differentiation under specific conditions*(34, 52)*. Our study is the first to provide evidence that exogenous human EG give rise to neurons in the injured brain. Evaluation at earlier time points would help to understand the fate of hEG after intranasal administration, when exactly neurons are generated, and what mechanisms regulate this process.

Noteworthy, hEG-derived mature neurons exhibited a high degree of integration into the brain cortex, revealing alignment within the host tissue. Furthermore, surrounding host oligodendrocytes myelinated the axons of hEG-derived neurons, and positive synaptophysin staining indicated that these neurons possessed the requisite components for establishing functional connections.

Overall, our study clearly demonstrated that hEG have a therapeutic potential, and can be safely used for brain regeneration strategies. This is the first study of its kind and has the potential to be a pivotal turning point in the field of regenerative medicine for brain injury.

Limitations: In our study, we could not assess whether hEG-derived neurons were functional. This type of investigation necessitates the utilization of innovative methodologies and the capacity to label hEG using fluorescent reporters to xenografting, thereby enabling real-time tracing of transplanted cells. Further research is required to eventually identify the subtypes of hEG-derived neurons. Moreover, it would be beneficial for future studies to extend the observation period to understand the dynamics of hEG fate and their long-term impact on brain repair and functional recovery.

METHODS

Animals

The study involved 28 female Sprague-Dawley rats (280 to 320g, 11 weeks old, Janvier, France). They were housed in pairs (cage size: 30 cm in length, 18 cm height, 32 cm width) in a controlled environment (20°C) with a 12h/12h light/dark cycle and had free access to food and water. The protocol was approved by the "*Direction Départementale de la Protection des Populations de la Haute – Garonne*" and the "*Comité d'éthique pour l'expérimentation animale Midi- Pyrénées*" (protocol n° APAFIS#22419 2019101115259327v5). Every effort was made to minimize the number of animals used and their distress. The animals were treated in accordance with the guidelines issued by the Council of the European Communities (EU Directive 2010/63). All the experiments have been reported following the ARRIVE guidelines. The animals were divided into four groups: rats receiving hEG *(n=7)*; rats receiving vehicle (PBS, *n=7*); rats receiving hEG-conditioned medium *(n=7*, "conditioned medium" in the text*)* and rats receiving medium alone (DMEM, *n=7*).

Brain injury induction

To induce brain injury, we used the malonate model, which has the advantage of targeting key brain regions involved in human ischemic stroke, such as the sensorimotor cortex*(24, 25, 53)*. Malonate interferes with the Krebs cycle and respiratory chain enzymes, thus creating a chemical energy failure. This mechanism is close to ischemia in that it induces an excitotoxic lesion with a penumbra*(54–57)*. Additionally, the malonate model is suitable for group comparisons in pharmacological studies involving time-consuming experiments (behavior, MRI, histology). The detailed description of brain injury induction is in *Supplementary files.*

Isolation, propagation, and cryopreservation of hEG

Human EG were isolated and propagated as we previously established*(15)* (detailed in *Supplementary Files*). Upon reaching confluence, the cultures were passaged every 7–10 days with trypsin (Sigma-Aldrich). At the third passage, the cultures were preserved in cryoprotectant medium (DMEM-F12 1:1 mixture, DMSO 10%) and transferred to liquid nitrogen. The cryovials were thawed and subsequently propagated (through two passages) two weeks prior to the intranasal delivery in rats. To ensure consistency, hEG were used at their fifth passage

throughout the study. This protocol enabled the desired number of cells to be obtained for transplantation.

Characterization of hEG cultures

Characterization of hEG cultures was performed by immunofluorescence. To this aim, the cells were placed in an 8-compartment LAB-TEK^{TM} slide culture chamber. They were washed with PBS 1X before fixation in paraformaldehyde (PFA) 4%, for 30 minutes at room temperature. PBS-Triton-X at 0.1 mol/L combined with 4% goat serum (blocking buffer) was used to mask non-specific binding sites for 2hrs at room temperature. Cells were then incubated overnight at 4°C with primary antibodies for glial, neuronal and fibroblast markers (Table 1). The cultures were then incubated for 2hrs at room temperature with respective secondary antibodies (Table1). The absence of non-specific labelling was ensured by negative controls.

Intranasal delivery in immunocompetent rats

Ten days after brain injury, rats received hEG *(n=7)* or vehicle (PBS, *n=7*), *via* the olfactory pathway*(58, 59)* using a 20 µl pipette with cone. Cell suspension was prepared as follows: 48hrs before intranasal delivery, hEG (passage fifth) were cultured in FCS-free medium (DMEM: F12 1:1 mixture). To avoid problems in interpreting the data from the administration of hEG from three patients, we decided to use hEG from one patient. The day of intranasal delivery, cells washed with sterile PBS 1X, trypsinised (Trypsin-EDTA solution 1X, Sigma-Aldrich), centrifuged at 1200 rpm for 5 min. Next, the supernatant was discarded and the cells were resuspended at a density of 2.5×10^5cells/60 µl in sterile PBS 1X. Thirty minutes prior to the administration of hEG, all animals were given 100 U hyaluronidase (Sigma-Aldrich) dissolved in sterile PBS 1X. Hyaluronidase was used here to disrupt the cells tight junction and the barrier function of the nasopharyngeal mucosa to facilitate the entry of the cells into the brain*(33, 44, 60)*. Rats were awake and held under the forelimb by an experimenter. Intranasal delivery was performed once a week for one month. Ten µl drops containing either hEG suspension or vehicle were placed at the edge of one nostril and instilled (10 µl per nostril, three times, 60 µl/week). At the end of the treatment, a total volume of 240 µl of cell suspension (1×10^6 cells) or vehicle was used, per animal. The volume and cell number were optimized and chosen based on the literature, to be effective in delivering cells into the brain through the cribriform plate *(33, 42, 61, 62)*. In parallel, a third and fourth group of rats received conditioned medium *(n=7)* or

medium alone (DMEM, *n=7*), respectively. In these groups, intranasal application was performed every day for one month (10 µl per nostril, three times, 60 µl/day). At the end of the treatment, a total volume of 600 µl of conditioned medium, or medium, were used. The experimenters were blinded to treatment throughout the whole study.

Behavioral Tests

To assess sensorimotor function, rats were trained to perform a grip strength test and neurologic severity score two weeks before surgery. Behavioral tests were performed one week before injury (baseline), then 48 hours after injury, weekly for the first month, and monthly for the following six months. Each time point was assessed in triplicate on three different days within the same week. The limb-use asymmetry test and the light-dark box test were two additional tests used in the study. These were performed eight times: one week pre-injury, and then one, four, eight, twelve, sixteen, twenty-, and twenty-four-weeks post-injury. The detailed description of behavioral tests is in *Supplementary files*.

Histological analysis of brain slices

The brain tissue was processed to evaluate tissue anatomy, remodeling, and new tissue formation thirty-six weeks post-injury, which corresponds to thirty-two weeks after hEG intranasal delivery. Nissl staining was used to evaluate tissue regeneration, while staining with specific markers was performed to identify human donor and host cells (Table 2 and *Supplementary M&M*).

Statistical Analysis

Comparisons between two groups were performed using the Mann-Whitney U-test. Paired repeated measures were analyzed using the mixed-effects analysis multiple comparison with Bonferroni correction. We used an unpaired t-test with a 95% confidence interval, after checking (with residual analysis) for equal variances between the different groups. Results were presented as median and the interquartile range (first quartile Q1; third quartile Q3). GraphPad Prism software was used for statistical analysis. Investigators were blinded to the treatment throughout the study.

Acknowledgements:

We thank Dr Costanza Simoncini for precious help in MRI data analysis, and Mr David Sagnat for technical assistance with human samples. We thank the Non-Invasive Exploration Service,

the Experimental Histopathology Platform, and the Animal Experiment Facilities of the US006/CREFRE-Anexplo, Inserm/UT3/ENVT; the Image Core Facility of the Infinity Institute (Inserm) headed by Sophie Allart. We are grateful to Prof Hideki Enomoto and Dr Mukhamad Sunardi (Kobe University, Japan), Dr Vassilis Pachnis and Dr Anna Laddach (The Crick Institute, London, UK), and Dr Alice Le Friec (Toulouse University) for their valuable advice.

Author contribution:

N.C.: conceptualization, experiments, data analysis, writing original manuscript; E.R.: experiments, data analysis; F.D.: MRI acquisition and analysis, editing; M.C. and M.P.: experiments; L.R.: technical help; E.B. and B. B.: surgical resection of human intestinal tissue; N.V.: responsible for human sample collection, editing; I.R.L.: experiments, data analysis, editing; I.L.: funding acquisition, editing; C.C.: conceptualization, experiments, data analysis, writing original manuscript, supervision, funding acquisition.

Funding:

N.C. is supported by the Foundation “Gueules Cassées” (Grant numbers 24-2021, 22-2022, 11-2023, 18-2024). We thank the Foundation “Gueules Cassées” (Grant numbers 17-2024 to CC; 55-2021 to IL) and the National Research Agency (ANR) (Grant number ANR-19-ASTR-0027 to CC and IL) for financial support.

Conflict of Interest:

Nothing to disclose.

REFERENCES

1. C. Cirillo, N. Brihmat, E. Castel-Lacanal, A. Le Friec, M. Barbieux-Guillot, N. Raposo, J. Pariente, A. Viguier, M. Simonetta-Moreau, J.-F. Albucher, J.-M. Olivot, F. Desmoulin, P. Marque, F. Chollet, I. Loubinoux, Post-stroke remodeling processes in animal models and humans. *J. Cereb. Blood Flow Metab. Off. J. Int. Soc. Cereb. Blood Flow Metab.* **40**, 3–22 (2020).

2. Z. Kokaia, I. L. Llorente, S. T. Carmichael, Customized Brain Cells for Stroke Patients Using Pluripotent Stem Cells. *Stroke* **49**, 1091–1098 (2018).

3. R. E. Sandu, A. T. Balseanu, C. Bogdan, M. Slevin, E. Petcu, A. Popa-Wagner, Stem cell therapies in preclinical models of stroke. Is the aged brain microenvironment refractory to cell therapy? *Exp. Gerontol.* **94**, 73–77 (2017).

4. F. Laso-García, L. Diekhorst, M. C. Gómez-de Frutos, L. Otero-Ortega, B. Fuentes, G. Ruiz-Ares, E. Díez-Tejedor, M. Gutiérrez-Fernández, Cell-Based Therapies for Stroke: Promising Solution or Dead End? Mesenchymal Stem Cells and Comorbidities in Preclinical Stroke Research. *Front. Neurol.* **10**, 332 (2019).

5. X.-L. Zhang, X.-G. Zhang, Y.-R. Huang, Y.-Y. Zheng, P.-J. Ying, X.-J. Zhang, X. Lu, Y.-J. Wang, G.-Q. Zheng, Stem Cell-Based Therapy for Experimental Ischemic Stroke: A Preclinical Systematic Review. *Front. Cell. Neurosci.* **15**, 628908 (2021).

6. C. V. Borlongan, Concise Review: Stem Cell Therapy for Stroke Patients: Are We There Yet? *STEM CELLS Transl. Med.* , sctm.19-0076 (2019).

7. R. Rust, C. Tackenberg, Stem Cell Therapy for Repair of the Injured Brain: Five Principles. *Neurosci. Rev. J. Bringing Neurobiol. Neurol. Psychiatry* **30**, 10–16 (2024).

8. K. Takahashi, K. Tanabe, M. Ohnuki, M. Narita, T. Ichisaka, K. Tomoda, S. Yamanaka, Induction of pluripotent stem cells from adult human fibroblasts by defined factors. *Cell* **131**, 861–872 (2007).

9. K. Miura, Y. Okada, T. Aoi, A. Okada, K. Takahashi, K. Okita, M. Nakagawa, M. Koyanagi, K. Tanabe, M. Ohnuki, D. Ogawa, E. Ikeda, H. Okano, S. Yamanaka, Variation in the safety of induced pluripotent stem cell lines. *Nat. Biotechnol.* **27**, 743–745 (2009).

10. H. Kawai, T. Yamashita, Y. Ohta, K. Deguchi, S. Nagotani, X. Zhang, Y. Ikeda, T. Matsuura, K. Abe, Tridermal Tumorigenesis of Induced Pluripotent Stem Cells Transplanted in Ischemic Brain. *J. Cereb. Blood Flow Metab.* **30**, 1487–1493 (2010).

11. Q. Vu, K. Xie, M. Eckert, W. Zhao, S. C. Cramer, Meta-analysis of preclinical studies of mesenchymal stromal cells for ischemic stroke. *Neurology* **82**, 1277–1286 (2014).

12. M. H. Amer, F. R. A. J. Rose, K. M. Shakesheff, M. Modo, L. J. White, Translational considerations in injectable cell-based therapeutics for neurological applications: concepts, progress and challenges. *Npj Regen. Med.* **2**, 23 (2017).

13. G. Mangin, N. Kubis, Cell Therapy for Ischemic Stroke: How to Turn a Promising Preclinical Research into a Successful Clinical Story. *Stem Cell Rev. Rep.* **15**, 176–193 (2019).

14. J. B. Furness, The enteric nervous system and neurogastroenterology. *Nat. Rev. Gastroenterol. Hepatol.* **9**, 286–294 (2012).

15. C. Cirillo, G. Sarnelli, F. Turco, A. Mango, M. Grosso, G. Aprea, S. Masone, R. Cuomo, Proinflammatory stimuli activates human-derived enteroglial cells and induces autocrine nitric oxide production. *Neurogastroenterol. Motil.* **23**, e372-382 (2011).

16. G. Esposito, C. Cirillo, G. Sarnelli, D. De Filippis, F. P. D'Armiento, A. Rocco, G. Nardone, R. Petruzzelli, M. Grosso, P. Izzo, T. Iuvone, R. Cuomo, Enteric Glial-Derived S100B Protein Stimulates Nitric Oxide Production in Celiac Disease. *Gastroenterology* **133** (2007), doi:10.1053/j.gastro.2007.06.009.

17. C. Cirillo, G. Sarnelli, G. Esposito, M. Grosso, R. Petruzzelli, P. Izzo, G. Calì, F. P. D'Armiento, A. Rocco, G. Nardone, T. Iuvone, L. Steardo, R. Cuomo, Increased mucosal nitric oxide production in ulcerative colitis is mediated in part by the enteroglial-derived S100B protein. *Neurogastroenterol. Motil.* **21** (2009), doi:10.1111/j.1365-2982.2009.01346.x.

18. W. Boesmans, C. Cirillo, V. Van den Abbeel, C. Van den Haute, I. Depoortere, J. Tack, P. Vanden Berghe, Neurotransmitters involved in fast excitatory neurotransmission directly activate enteric glial cells. *Neurogastroenterol. Motil.* **25** (2013), doi:10.1111/nmo.12065.

19. C. Cirillo, T. Bessissow, A. S. Desmet, H. Vanheel, J. Tack, P. V. Berghe, Evidence for neuronal and structural changes in submucous ganglia of patients with functional dyspepsia. *Am. J. Gastroenterol.* **110**, 1205–1215 (2015).

20. A. Liñán-Rico, F. Turco, F. Ochoa-Cortes, A. Harzman, B. J. Needleman, R. Arsenescu, M. Abdel-Rasoul, P. Fadda, I. Grants, E. Whitaker, R. Cuomo, F. L. Christofi, Molecular Signaling and Dysfunction of the Human Reactive Enteric Glial Cell Phenotype: Implications for GI Infection, IBD, POI, Neurological, Motility, and GI Disorders. *Inflamm. Bowel Dis.* **22**, 1812–1834 (2016).

21. C. Pochard, S. Coquenlorge, J. Jaulin, N. Cenac, N. Vergnolle, G. Meurette, M. Freyssinet, M. Neunlist, M. Rolli-Derkinderen, Defects in 15-HETE Production and Control of Epithelial Permeability by Human Enteric Glial Cells from Patients with Crohn's Disease. *Gastroenterology* **150**, 168–180 (2016).

22. S. Hacene, A. Le Friec, F. Desmoulin, L. Robert, N. Colitti, J. Fitremann, I. Loubinoux, C. Cirillo, Present and future avenues of cell-based therapy for brain injury: The enteric nervous system as a potential cell source. *Brain Pathol.* **32**, e13105 (2022).

23. N. Colitti, F. Desmoulin, A. Le Friec, W. Labriji, L. Robert, A. Michaux, F. Conchou, C. Cirillo, I. Loubinoux, Long-Term Intranasal Nerve Growth Factor Treatment Favors Neuron Formation in de novo Brain Tissue. *Front. Cell. Neurosci.* **16**, 871532 (2022).

24. C. Davoust, B. Plas, A. Béduer, B. Demain, A.-S. Salabert, J.-C. C. Sol, C. Vieu, L. Vaysse, I. Loubinoux, Regenerative potential of primary adult human neural stem cells on micropatterned bioimplants boosts motor recovery. *Stem Cells Res. Ther.* **8**, 253 (2017).

25. L. Vaysse, F. Conchou, B. Demain, C. Davoust, B. Plas, C. Ruggieri, M. Benkaddour, M. Simonetta-Moreau, I. Loubinoux, Strength and fine dexterity recovery profiles after a primary motor cortex insult and effect of a neuronal cell graft. *Behav. Neurosci.* **129**, 423–434 (2015).

26. K. D. Beck, H. X. Nguyen, M. D. Galvan, D. L. Salazar, T. M. Woodruff, A. J. Anderson, Quantitative analysis of cellular inflammation after traumatic spinal cord injury: evidence for a multiphasic inflammatory response in the acute to chronic environment. *Brain J. Neurol.* **133**, 433–447 (2010).

27. M. Daglas, D. F. Draxler, H. Ho, F. McCutcheon, A. Galle, A. E. Au, P. Larsson, J. Gregory, F. Alderuccio, M. Sashindranath, R. L. Medcalf, Activated CD8+ T Cells Cause Long-Term Neurological Impairment after Traumatic Brain Injury in Mice. *Cell Rep.* **29**, 1178-1191.e6 (2019).

28. Y. Shinozaki, K. Shibata, K. Yoshida, E. Shigetomi, C. Gachet, K. Ikenaka, K. F. Tanaka, S. Koizumi, Transformation of Astrocytes to a Neuroprotective Phenotype by Microglia via P2Y1 Receptor Downregulation. *Cell Rep.* **19**, 1151–1164 (2017).

29. S. Okada, M. Nakamura, H. Katoh, T. Miyao, T. Shimazaki, K. Ishii, J. Yamane, A. Yoshimura, Y. Iwamoto, Y. Toyama, H. Okano, Conditional ablation of Stat3 or Socs3 discloses a dual role for reactive astrocytes after spinal cord injury. *Nat. Med.* **12**, 829–834 (2006).

30. M. A. Anderson, T. M. O'Shea, J. E. Burda, Y. Ao, S. L. Barlatey, A. M. Bernstein, J. H. Kim, N. D. James, A. Rogers, B. Kato, A. L. Wollenberg, R. Kawaguchi, G. Coppola, C. Wang, T. J. Deming, Z. He, G. Courtine, M. V. Sofroniew, Required growth facilitators propel axon regeneration across complete spinal cord injury. *Nature* **561**, 396–400 (2018).

31. L. Danielyan, S. Beer-Hammer, A. Stolzing, R. Schäfer, G. Siegel, C. Fabian, P. Kahle, T. Biedermann, A. Lourhmati, M. Buadze, A. Novakovic, B. Proksch, C. H. Gleiter, W. H. Frey, M. Schwab, Intranasal Delivery of Bone Marrow-Derived Mesenchymal Stem Cells, Macrophages, and Microglia to the Brain in Mouse Models of Alzheimer's and Parkinson's Disease. *Cell Transplant.* **23**, 123–139 (2014).

32. L. Danielyan, R. Schäfer, A. von Ameln-Mayerhofer, M. Buadze, J. Geisler, T. Klopfer, U. Burkhardt, B. Proksch, S. Verleysdonk, M. Ayturan, G. H. Buniatian, C. H. Gleiter, W. H. Frey, Intranasal delivery of cells to the brain. *Eur. J. Cell Biol.* **88**, 315–324 (2009).

33. B. Parajuli, H. Saito, Y. Shinozaki, E. Shigetomi, H. Miwa, S. Yoneda, M. Tanimura, S. Omachi, T. Asaki, K. Takahashi, M. Fujita, K. Nakashima, S. Koizumi, Transnasal transplantation of human induced pluripotent stem cell-derived microglia to the brain of immunocompetent mice. *Glia* **69**, 2332–2348 (2021).

34. A. Laddach, S. H. Chng, R. Lasrado, F. Progatzky, M. Shapiro, A. Erickson, M. Sampedro Castaneda, A. V. Artemov, A. C. Bon-Frauches, E.-M. Amaniti, J. Kleinjung, S. Boeing, S. Ultanir, I. Adameyko, V. Pachnis, A branching model of lineage differentiation underpinning the neurogenic potential of enteric glia. *Nat. Commun.* **14**, 5904 (2023).

35. L. Huang, Z.-B. Wu, Q. ZhuGe, W. Zheng, B. Shao, B. Wang, F. Sun, K. Jin, Glial Scar Formation Occurs in the Human Brain after Ischemic Stroke. *Int. J. Med. Sci.* **11**, 344–348 (2014).

36. M. L. Cotrina, N. Lou, J. Tome-Garcia, J. Goldman, M. Nedergaard, Direct comparison of microglial dynamics and inflammatory profile in photothrombotic and arterial occlusion evoked stroke. *Neuroscience* **343**, 483–494 (2017).

37. N. A. Flaris, T. L. Densmore, M. C. Molleston, W. F. Hickey, Characterization of microglia and macrophages in the central nervous system of rats: definition of the differential expression of molecules

using standard and novel monoclonal antibodies in normal CNS and in four models of parenchymal reaction. *Glia* **7**, 34–40 (1993).

38. M. Koshinaga, Y. Katayama, M. Fukushima, H. Oshima, T. Suma, T. Takahata, Rapid and widespread microglial activation induced by traumatic brain injury in rat brain slices. *J. Neurotrauma* **17**, 185–192 (2000).

39. M. Meir, S. Flemming, N. Burkard, L. Bergauer, M. Metzger, C. T. Germer, N. Schlegel, Glial cell line-derived neurotrophic factor promotes barrier maturation and wound healing in intestinal epithelial cells in vitro. *Am. J. Physiol. - Gastrointest. Liver Physiol.* **309**, G613–G624 (2015).

40. A. Contestabile, R. Colangiulo, M. Lucchini, A.-D. Gindrat, A. Hamadjida, M. Kaeser, J. Savidan, A. F. Wyss, E. M. Rouiller, E. Schmidlin, Asymmetric and Distant Effects of a Unilateral Lesion of the Primary Motor Cortex on the Bilateral Supplementary Motor Areas in Adult Macaque Monkeys. *J. Neurosci.* **38**, 10644–10656 (2018).

41. P. R. Vehrs, M. Uvacsek, A. W. Johnson, Assessment of Dysfunctional Movements and Asymmetries in Children and Adolescents Using the Functional Movement Screen—A Narrative Review. *Int. J. Environ. Res. Public. Health* **18**, 12501 (2021).

42. M. J. Chau, T. C. Deveau, X. Gu, Y. S. Kim, Y. Xu, S. P. Yu, L. Wei, Delayed and repeated intranasal delivery of bone marrow stromal cells increases regeneration and functional recovery after ischemic stroke in mice. *BMC Neurosci.* **19**, 20 (2018).

43. M.-H. Lu, W.-L. Ji, H. Chen, Y.-Y. Sun, X.-Y. Zhao, F. Wang, Y. Shi, Y.-N. Hu, B.-X. Liu, J. Wu, D.-E. Xu, J.-W. Zheng, C.-F. Liu, Q.-H. Ma, Intranasal Transplantation of Human Neural Stem Cells Ameliorates Alzheimer's Disease-Like Pathology in a Mouse Model. *Front. Aging Neurosci.* **13**, 650103 (2021).

44. L. Danielyan, S. Beer-Hammer, A. Stolzing, R. Schäfer, G. Siegel, C. Fabian, P. Kahle, T. Biedermann, A. Lourhmati, M. Buadze, A. Novakovic, B. Proksch, C. H. Gleiter, W. H. Frey, M. Schwab, Intranasal Delivery of Bone Marrow-Derived Mesenchymal Stem Cells, Macrophages, and Microglia to the Brain in Mouse Models of Alzheimer's and Parkinson's Disease. *Cell Transplant.* **23**, 123–139 (2014).

45. H. Shen, X. Gu, Z. Z. Wei, A. Wu, X. Liu, L. Wei, Combinatorial intranasal delivery of bone marrow mesenchymal stem cells and insulin-like growth factor-1 improves neurovascularization and functional outcomes following focal cerebral ischemia in mice. *Exp. Neurol.* **337**, 113542 (2021).

46. V. Donega, C. H. Nijboer, L. Braccioli, I. Slaper-Cortenbach, A. Kavelaars, F. Van Bel, C. J. Heijnen, P. Gressens, Ed. Intranasal Administration of Human MSC for Ischemic Brain Injury in the Mouse: In Vitro and In Vivo Neuroregenerative Functions. *PLoS ONE* **9**, e112339 (2014).

47. Y. Sato, N. Shinjyo, M. Sato, M. K. L. Nilsson, K. Osato, C. Zhu, M. Pekna, H. G. Kuhn, K. Blomgren, Grafting Neural Stem and Progenitor Cells Into the Hippocampus of Juvenile, Irradiated Mice Normalizes Behavior Deficits. *Front. Neurol.* **9** (2018), doi:10.3389/fneur.2018.00715.

48. A. M. Osman, K. Zhou, C. Zhu, K. Blomgren, Transplantation of enteric neural stem/progenitor cells into the irradiated young mouse hippocampus. *Cell Transplant.* **23**, 1657–1671 (2014).

49. J. Belkind-Gerson, R. Hotta, M. Whalen, N. Nayyar, N. Nagy, L. Cheng, A. Zuckerman, A. M. Goldstein, J. Dietrich, Engraftment of enteric neural progenitor cells into the injured adult brain. *BMC Neurosci.* **17**, 5 (2016).

50. R. Stavely, R. Hotta, N. Picard, A. A. Rahman, W. Pan, S. Bhave, M. Omer, W. L. N. Ho, R. A. Guyer, A. M. Goldstein, Schwann cells in the subcutaneous adipose tissue have neurogenic potential and can be used for regenerative therapies. *Sci. Transl. Med.* **14**, eabl8753 (2022).

51. S. Hetz, A. Acikgoez, U. Voss, K. Nieber, H. Holland, C. Hegewald, H. Till, R. Metzger, M. Metzger, In Vivo Transplantation of Neurosphere-Like Bodies Derived from the Human Postnatal and Adult Enteric Nervous System: A Pilot Study. *PLOS ONE* **9**, e93605 (2014).

52. C. Laranjeira, K. Sandgren, N. Kessaris, W. Richardson, A. Potocnik, P. Vanden Berghe, V. Pachnis, Glial cells in the mouse enteric nervous system can undergo neurogenesis in response to injury. *J. Clin. Invest*. **121**, 3412–3424 (2011).

53. L. Vaysse, A. Beduer, J. C. Sol, C. Vieu, I. Loubinoux, Micropatterned bioimplant with guided neuronal cells to promote tissue reconstruction and improve functional recovery after primary motor cortex insult. *Biomaterials* **58**, 46–53 (2015).

54. L. Barros-Miñones, L. Orejana, B. Goñi-Allo, V. Suquía, I. Hervías, N. Aguirre, E. Puerta, Modulation of the ASK1-MKK3/6-p38/MAPK signalling pathway mediates sildenafil protection against chemical hypoxia caused by malonate: Sildenafil and chemical hypoxia. *Br. J. Pharmacol.* **168**, 1820–1834 (2013).

55. D. J. Cuthill, J. H. Fowler, J. McCulloch, D. Dewar, Different patterns of axonal damage after intracerebral injection of malonate or AMPA. *Exp. Neurol.* **200**, 509–520 (2006).

56. J. G. Greene, J. T. Greenamyre, Exacerbation of NMDA, AMPA, and l-Glutamate Excitotoxicity by the Succinate Dehydrogenase Inhibitor Malonate. *J. Neurochem.* **64**, 2332–2338 (2002).

57. R. Henshaw, B. G. Jenkins, J. B. Schulz, R. J. Ferrante, N. W. Kowall, B. R. Rosen, M. Flint Beal, Malonate produces striatal lesions by indirect NMDA receptor activation. *Brain Res.* **647**, 161–166 (1994).

58. C. Galeano, Z. Qiu, A. Mishra, S. L. Farnsworth, J. J. Hemmi, A. Moreira, P. Edenhoffer, P. J. Hornsby, The Route by Which Intranasally Delivered Stem Cells Enter the Central Nervous System. *Cell Transplant.* **27**, 501–514 (2018).

59. M. S. Salehi, B. Jurek, S. Karimi-Haghighi, N. J. Nezhad, S. M. Mousavi, E. Hooshmandi, A. Safari, M. Dianatpour, S. Haerteis, J. A. Miyan, S. Pandamooz, A. Borhani-Haghighi, Intranasal application of stem cells and their derivatives as a new hope in the treatment of cerebral hypoxia/ischemia: a review. *Rev. Neurosci.* **33**, 583–606 (2022).

60. L. Danielyan, R. Schäfer, A. von Ameln-Mayerhofer, M. Buadze, J. Geisler, T. Klopfer, U. Burkhardt, B. Proksch, S. Verleysdonk, M. Ayturan, G. H. Buniatian, C. H. Gleiter, W. H. Frey, Intranasal delivery of cells to the brain. *Eur. J. Cell Biol.* **88**, 315–324 (2009).

61. T. Inoue, M. Sugiyama, H. Hattori, H. Wakita, T. Wakabayashi, M. Ueda, Stem Cells from Human Exfoliated Deciduous Tooth-Derived Conditioned Medium Enhance Recovery of Focal Cerebral Ischemia in Rats. *Tissue Eng. Part A* **19**, 24–29 (2013).

62. J. Sun, Z. Z. Wei, X. Gu, J. Y. Zhang, Y. Zhang, J. Li, L. Wei, Intranasal delivery of hypoxia-preconditioned bone marrow-derived mesenchymal stem cells enhanced regenerative effects after intracerebral hemorrhagic stroke in mice. *Exp. Neurol.* **272**, 78–87 (2015).